

# Enzymatic Cascade Reactions inside Polymeric Nanocontainers: A Means to Combat Oxidative Stress

Pascal Tanner, Ozana Onaca, Vimalkumar Balasubramanian, Wolfgang Meier, and  
Cornelia G. Palivan\*<sup>[a]</sup>

**Abstract:** Oxidative stress, which is primarily due to an imbalance in reactive oxygen species, such as superoxide radicals, peroxyxynitrite, or hydrogen peroxide, represents a significant initiator in pathological conditions that range from arthritis to cancer. Herein we introduce the concept of enzymatic cascade reactions inside polymeric nanocontainers as an effective means to detect and combat superoxide radicals. By simultaneously encapsulating a set of enzymes that act in tandem inside the cavities of polymeric nanovesicles and by reconstituting channel proteins in

their membranes, an efficient catalytic system was formed, as demonstrated by fluorescence correlation spectroscopy and fluorescence cross-correlation spectroscopy. Superoxide dismutase and lactoperoxidase were selected as a model to highlight the combination of enzymes. These were shown to participate in sequential reactions in situ in the nanovesicle cavity, transforming su-

peroxide radicals to molecular oxygen and water and, therefore, mimicking their natural behavior. A channel protein, outer membrane protein F, facilitated the diffusion of lactoperoxidase substrate/products and dramatically increased the penetration of superoxide radicals through the polymer membrane, as established by activity assays. The system remained active after uptake by THP-1 cells, thus behaving as an artificial organelle and exemplifying an effective approach to enzyme therapy.

**Keywords:** artificial organelles • enzyme catalysis • nanostructures • oxidative stress • self-assembly

## Introduction

A key challenge in the life- and nanosciences is fusing biological entities, such as enzymes, with synthetic materials, for example, block copolymers, to create new, complex synthetic biological devices.<sup>[1,2]</sup> Combining the specificity and efficiency of biological molecules with the robustness and possibility of tailoring polymeric materials allows the design of efficient mimics of living entities. These outperform conventional chemical or biological approaches to generate revolutionary, highly specific communicating or processing systems, such as biosensors, signal amplifiers, electron-transfer devices, or nanoreactors.<sup>[3–5]</sup> Enzymatic activity can be improved and enzymatic pathways customized by combining synthetic with biological materials, as shown by trypsin encapsulation in PS-*b*-PAA block copolymers<sup>[6]</sup> or by reconstitution of ubiquinone oxidoreductase in copolymer membranes.<sup>[7]</sup> However, a real challenge is related to the preservation of enzyme activity and integrity when combined with polymeric systems. This renders the situation far more complex than in bulk conditions, and requires mild procedures

to generate hybrid systems and the ascertainment of polymer–protein interactions and their effects on enzyme structure and activity.

Recently such biosynthetic materials were successfully applied to local bioconversion on surfaces<sup>[8]</sup> and inside living cells.<sup>[9]</sup> Herein we plan to extend these concepts to the detoxification of reactive oxygen species (ROS), including the superoxide radical anion ( $O_2^{\cdot-}$ ), peroxyxynitrite, hydroxyl radical, and hydrogen peroxide, the natural production of which is dramatically increased during oxidative stress.<sup>[10]</sup> The imbalance in ROS, which characterizes oxidative stress, overwhelms cellular antioxidant defense mechanisms, including glutathione peroxidase, glutathione transferase, catalase, and superoxide dismutase (SOD). Such an imbalance has been reported to play an important role in both the toxicology of inorganic nanoparticles<sup>[11]</sup> and the pathogenesis of many diseases, such as arthritis, Parkinson's disease, cancer, and AIDS.<sup>[12–14]</sup> Attempts have been made to detoxify ROS by direct antioxidant enzyme administration, but this provided rather modest protection, if any, as reported for example for SOD, which was quickly eliminated from the bloodstream (6 min in rats and 30 min in humans).<sup>[15]</sup> Many efforts have been made to improve SOD delivery by covalent modification with polyethylene glycol (PEG)<sup>[16]</sup> or encapsulation into liposomes<sup>[17,18]</sup> or polymeric microspheres.<sup>[19]</sup> However, neither modification with PEG nor the use of conventional drug delivery approaches, in which the enzyme acts only after its release from the carrier, improved delivery significantly. This is due to inherent drawbacks, such as possible

[a] P. Tanner, Dr. O. Onaca, V. Balasubramanian, Prof. W. Meier, Priv. Doz. Dr. C. G. Palivan  
Department of Chemistry, University of Basel  
Klingelbergstrasse 80, 4056 Basel (Switzerland)  
Fax: (+41) 61-267-38-55  
E-mail: cornelia.palivan@unibas.ch

Supporting information for this article is available on the WWW under <http://dx.doi.org/10.1002/chem.201002782>.

deactivation of the enzyme by extensive modification,<sup>[20]</sup> significant leakage from liposomes due to structural defects, mechanical instability or short circulation lifetime,<sup>[21]</sup> and poor control of release from the polymer microspheres.<sup>[22]</sup> A further step was taken through the design of an antioxidant nanoreactor.<sup>[23]</sup> Nanoreactors are formed by encapsulation of active compounds inside polymeric vesicles,<sup>[24]</sup> in which they can simultaneously act in situ and are protected from proteolytic attack.<sup>[25,26]</sup> Various types of nanoreactors have been developed recently, either by changing the chemical nature of block copolymers or the enzyme/combination of enzymes to address applications in areas such as catalysis or therapeutics.<sup>[3,6,8,27]</sup> In this respect antioxidant nanoreactors have been used to encapsulate SOD inside oxygen-permeable polymeric vesicles in which the enzyme was able to catalyze the reaction of superoxide radicals.<sup>[23]</sup> However, the reaction generated hydrogen peroxide as a final product, which is known to contribute to oxidative damage.<sup>[28]</sup>

If detoxification of superoxide radicals and related harmful hydrogen peroxide is intended, as in cellular antioxidant mechanisms, a more complex system has to be designed. Herein we introduce the concept of enzymatic cascade reactions inside polymeric nanocontainers that detect and completely detoxify superoxide radicals to give water and molecular oxygen. This is based on coencapsulating in polymeric vesicles two enzymes known to act in tandem and to catalyze the reactions of the superoxide radicals in nature. The concept brings together the specificity, rapidity, and activity of a combination of enzymes that mimics cells conditions with the architecture and stability of self-assembled copolymer containers and results in a processor-like system. When superoxide radicals ambient to the polymer vesicles penetrate the synthetic membrane they encounter the combined enzymes, which act in a cascade reaction that leads to the harmless reaction products H<sub>2</sub>O and oxygen (Figure 1).

This concept was implemented with SOD and lactoperoxidase (LPO) as a model of enzymes that act in tandem. These were coencapsulated in the cavities of polymeric vesicles formed by the self-assembly of amphiphilic poly(2-methylloxazoline)-poly-(dimethylsiloxane)-poly(2-methyllox-

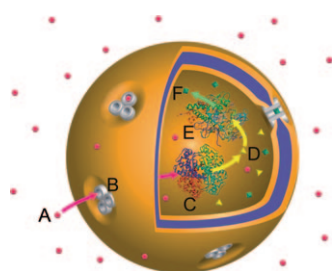


Figure 1. Schematic representation of enzymatic cascade reactions inside polymeric nanocontainers as a means to detect and combat oxidative stress. A combination of enzymes (C and E) act inside polymeric nanocontainers in a cascade reaction with substrates (D) and products (F) to detoxify reactive oxygen species (A). Substrates, products, and reactive oxygen species penetrate the polymeric membrane due to the insertion of protein channels (B).

azoline) (PMOXA-PDMS-PMOXA) triblock copolymers in aqueous solution at physiological pH. Using amphiphilic copolymers that self-assemble in aqueous solutions into vesicular structures, in a fashion analogous to lipids,<sup>[29]</sup> is a straightforward approach to simultaneously prepare polymeric vesicles and encapsulate enzymes inside.<sup>[25]</sup> We chose these amphiphilic block copolymers because they show good biocompatibility<sup>[30]</sup> and improved stability to lysis by classical surfactants as compared with liposomes.<sup>[17]</sup> The polymer membrane is highly impermeable to small molecules, such as water or sucrose,<sup>[31]</sup> whereas it is permeable to superoxide radicals.<sup>[32]</sup> To function, polymeric vesicles that contain a combination of enzymes capable of detoxifying O<sub>2</sub><sup>•-</sup> also require membranes that permit the passage of the substrate and the product of the second enzyme. To achieve this, outer membrane protein F (OmpF) is reconstituted in the vesicle wall to permit passive diffusion of small molecules (< 600 Da)<sup>[33]</sup> and thus modulate the copolymer membrane permeability without reducing stability or losing encapsulated enzymes. In this way the enzymes remain permanently trapped inside the cavity, a condition comparable to a living cell, whereas substrates and products can pass through the vesicle membrane, facilitating in situ enzyme activity.<sup>[31,34]</sup> Part of this concept includes a simple fluorescent means to detect superoxide radicals and to test antioxidant activity inside cells. This is based on the formation of fluorescent products in situ during the second step of the cascade reaction as the substrate penetrates the cavity through the OmpF channels. When tested in THP-1 cells, the system behaves as if artificial organelles were present and allows both detection and in situ, instant, complete detoxification of superoxide radicals. The system supports a theranostic approach to oxidative stress.

## Results and Discussion

**Design of enzymatic cascade reactions inside polymeric nanocontainers for O<sub>2</sub><sup>•-</sup> radical detoxification:** By combining the desired enzymatic cascade reaction with the protection effect of polymeric nanocontainers, a processor system was designed to detect and detoxify superoxide radicals that pass through the polymer membrane so that only harmless products result (Figure 2A). The cascade reaction starts with SOD activity as one part of the natural antioxidant defense mechanism (Figure 2B, reaction 2); the enzyme quickly catalyses the reaction of superoxide radicals at a high turnover number and is not affected by pH changes from pH 6 to pH 9.<sup>[35]</sup> H<sub>2</sub>O<sub>2</sub>, as the only harmful product of the SOD reaction, is degraded in the second step of the cascade reaction by LPO in the presence of one of its specific substrates, amplex red (Figure 2B, reaction 3). We chose LPO as the second enzyme in the sequence of reactions because at physiological pH it still preserves 80% of its full activity at pH 5.3,<sup>[36]</sup> which makes it compatible with SOD. As the source of O<sub>2</sub><sup>•-</sup>, we used the known combination of xanthine/xanthine oxidase, XA/XO (Figure 2B, reaction 1). The per-

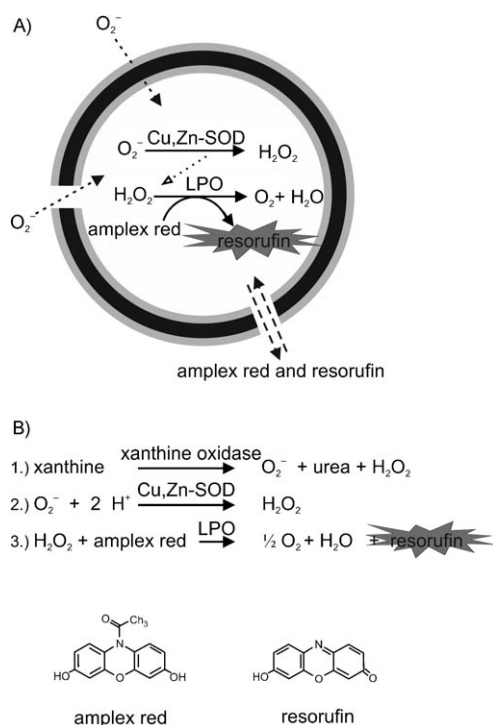


Figure 2. Design of the enzymatic cascade reaction inside polymeric nanocontainers for detection and superoxide radical detoxification. A) Schematic illustration of SOD–LPO cascade reaction inside a nanocontainer. B) Chemical reactions allowing the detection and detoxification of superoxide radicals: 1) generation of  $\text{O}_2^-$ ; 2) reactions involving SOD; 3) reactions involving LPO.

meability of the polymer membrane was modulated by insertion of OmpF channel proteins, which allowed only the passage of small molecules, such as amplex red and resorufin, the substrate/product of LPO. The amplex red and resorufin combination allows simple detection of  $\text{O}_2^-$  presence by a fluorescence signal generated in the last step of the cascade reaction.

#### Characterization of enzyme-containing polymeric vesicles:

The individual enzyme species and the combined enzymes were encapsulated whereas the channel protein was reconstituted during polymeric vesicle self-assembly. The encapsulation procedure involved dropwise addition of a solution of enzymes/protein to the copolymer with continuous stirring until the copolymer solution turned turbid, followed by the extrusion of the mixture. Knowledge of the physical dimensions and morphology (solid or hollow-sphere structure) is necessary to determine whether the presence of enzymes affects the self-assembly process of the vesicles. SOD-encapsulated-, LPO-encapsulated-, and SOD–LPO-encapsulated assemblies and empty polymer assemblies were, therefore, characterized with dynamic and static light-scattering and transmission electron microscopy (TEM).

Dynamic and static light-scattering experiments provided details on the types of objects formed by self-assembly in the presence of enzyme(s) and the size distribution and polydispersity (Supporting Information, Table S1). By divid-

ing the radius of gyration ( $R_G$ ) resulting from static light-scattering experiments by the hydrodynamic radius ( $R_H$ ) resulting from dynamic light-scattering,  $\rho = R_G/R_H$  (Supporting Information, Figures S1 and S2), values close to 1.0 were obtained both for empty vesicles and for those containing enzyme(s), which indicates hollow-sphere morphology. A mean polydispersity index of  $(0.26 \pm 0.09)$  was calculated. The form factor analysis<sup>[37]</sup> confirmed the model of hollow spheres as the most appropriate model for empty/enzyme-containing vesicles (Supporting Information, Figure S3). Variance of fit can most probably be explained by the polydispersity of the system. Although empty- and SOD-containing vesicles have similar hydrodynamic radii ( $\approx 160$  nm), coencapsulation of LPO and SOD was found to induce a decrease in size (to  $\approx 95$  nm). We assume this is due to interaction with the hydrophobic domain of the block copolymer. This effect depends on the amount of LPO. However, the values of  $\rho$  for LPO- and LPO–SOD-containing nanovesicles indicate the vesicular form of these assemblies. The values of the hydrodynamic radii of empty and SOD-containing vesicles are consistent with similar PMOXA-PDMS-based block copolymers with different hydrophobic-to-hydrophilic ratios.<sup>[31]</sup> Small values of the second virial coefficient  $A_2$  indicate an absence of long-range interactions between the vesicles in the investigated concentration range.

The TEM images reveal that the different vesicles have relatively uniform sizes. However, compared with light scattering, smaller, sphere-like objects were also imaged, which were anticipated as a result of the known deformation and shrinkage due to TEM sample preparation (Figure 3; Supporting Information, Figure S4). Together, light scattering and TEM prove that the presence of enzymes during the mild self-assembly encapsulation procedure does not affect vesicle formation.

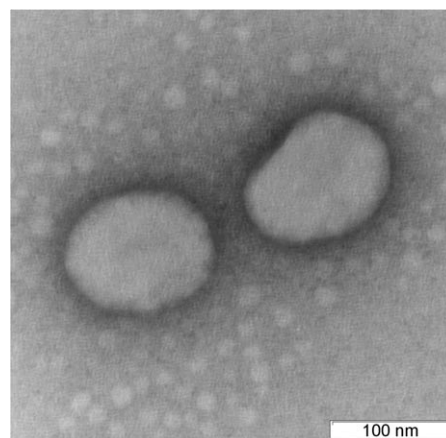


Figure 3. TEM image of PMOXA<sub>12</sub>-PDMS<sub>55</sub>-PMOXA<sub>12</sub> vesicles that contain a combination of SOD and LPO.

#### Encapsulation of individual enzyme species in nanovesicles:

The encapsulation of individual enzyme species in vesicles is necessary as a prerequisite for revealing the specific condi-

tions for coencapsulation of enzymes in a way that supports the cascade reaction. The encapsulation of each enzyme species was analyzed by using fluorescence correlation spectroscopy (FCS). Laser-induced fluorescence of molecules passing through a small confocal probe volume autocorrelates over time and provides information on the diffusion time of the molecule,  $\tau_D$ .<sup>[38]</sup> Differences in diffusion times are related to changes in the hydrodynamic radius by using the Stokes–Einstein relation, and permit a determination of interactions with larger assemblies, as is the case in ligand–protein interactions or encapsulation in polymeric systems.<sup>[23]</sup> Each enzyme was fluorescently labeled and encapsulated similarly to the unlabeled enzymes, to allow detection via FCS. The normalized FCS autocorrelation curves of enzyme-containing vesicle solutions were compared with those of free dye and free labeled enzyme (Figure 4A, B). Significant differences in the diffusion times were obtained. The  $\tau_D$  for Alexa488-SOD increased to 109  $\mu\text{s}$  compared with 29  $\mu\text{s}$  for free Alexa488,<sup>[39]</sup> corresponding to a hydrodynamic radius of 2.9 nm and consistent with the theoretical radius of 3 nm for an enzyme with a 33 kDa molecular mass. For encapsulated Alexa488-SOD, the multiphasic curve (Figure 4A, curve c)

indicates the presence of slowly diffusing particles. The best fit for the autocorrelation function of the time-dependent fluorescence signal (Supporting Information, Equation (2)) shows that two populations of particles were present after enzyme encapsulation. The major population (more than 80%), with a mean diffusion time of 2.5 ms, was attributed to SOD-Alexa488-containing vesicles, whereas the second population represents free dye not completely removed by dialysis.

To estimate the number of SOD molecules encapsulated in the nanovesicles, we compared the molecular brightness, reported as count rates per molecule (cpm, in kHz) of free dye, non-encapsulated Alexa488-SOD, and encapsulated Alexa488-SOD. We found that one Alexa488 is attached to one SOD molecule by using a calibration curve of molecular brightness as a function of the known concentrations of Alexa488. We took into account the effect of dye quenching due to conjugation of Alexa488 with SOD, which results in a decrease in molecular brightness from  $\text{cpm} = 32$  to 22 kHz. In the case of encapsulated Alexa488-SOD, the total molecular brightness ( $\text{cpm}_T$ ) corresponds to the weighted sum of the brightnesses of the individual components ( $\text{cpm}_i$ ). The

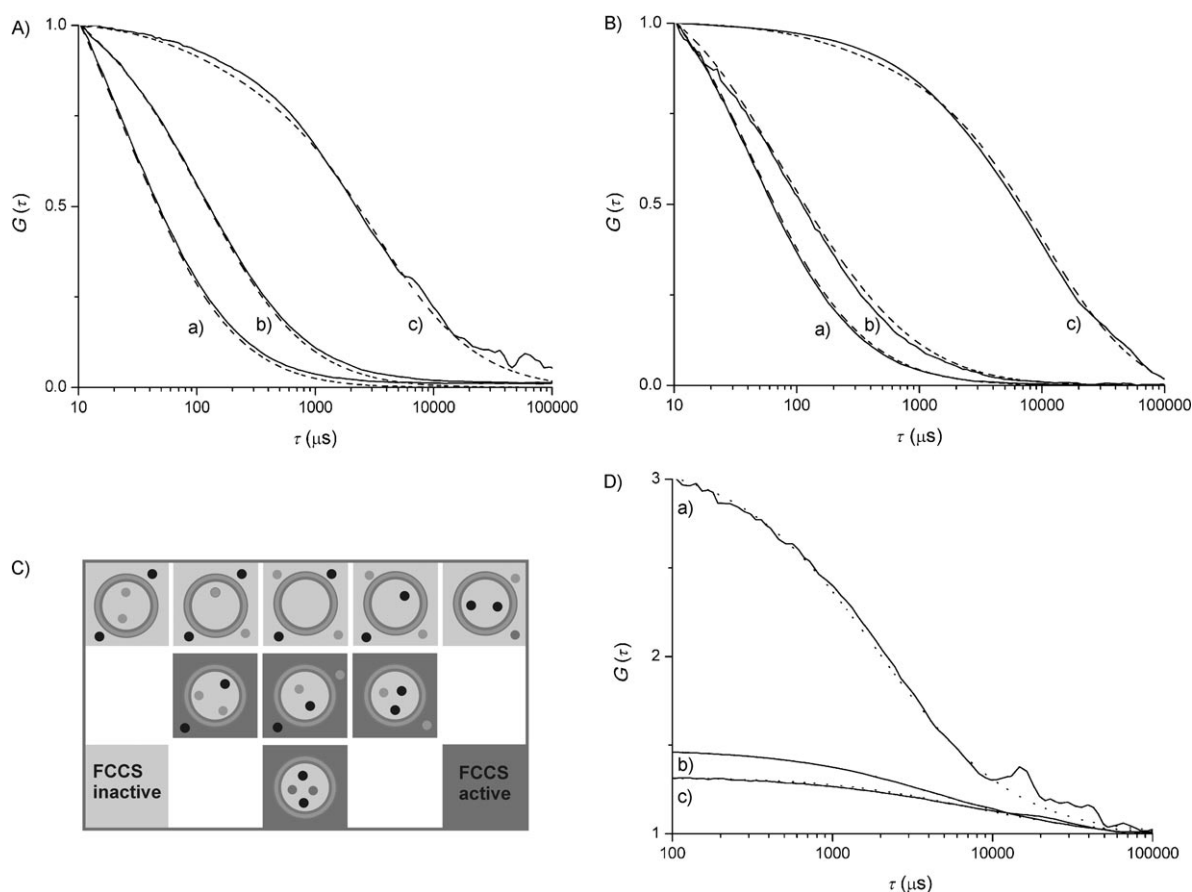


Figure 4. A) FCS autocorrelation curves and the simulation of free Alexa488 (a), Alexa488-SOD (b), and Alexa488-SOD-containing vesicles (c). B) FCS autocorrelation curves and the simulation of free Alexa633 (a), Alexa633-LPO (b), and Alexa633-LPO-containing nanovesicles (c). C) Scenario for the coexistence of vesicle populations that contain various encapsulated enzymes (●: Alexa488-SOD; ●: Alexa633-LPO) for a total number of four enzyme molecules. Only vesicles containing at least two different labeled enzymes are FCCS-active. D) FCCS/FCS curves of vesicles that contain Alexa488-SOD (autocorrelation curve; a), LPO-Alexa633 (autocorrelation curve; b), and a combination of Alexa488-SOD and LPO-Alexa633 (c). Dotted lines are fitted curves.

number of  $(4 \pm 3)$  SOD molecules per vesicle was obtained by dividing the molecular brightness of SOD-containing vesicles by the molecular brightness of freely diffusing Alexa488 for an initial labeled-enzyme concentration of  $0.5 \text{ mg mL}^{-1}$ . An encapsulation efficiency of approximately 23% was calculated by dividing the maximum possible number of SOD molecules (for an initial concentration of  $0.5 \text{ mg mL}^{-1}$ ) by the effective number of SOD molecules in a vesicle. Interestingly, similar values were obtained if SOD was encapsulated by using a different preparation procedure based on rehydration of the polymer film prior to the encapsulation.<sup>[32]</sup> This presents an opportunity to modulate the encapsulation procedure to cope with different copolymer properties, such as solubility.

On labeling LPO, the diffusion time of free dye increased from 51 to 322  $\mu\text{s}$ , which corresponds to 4 nm, consistent with the theoretical radius of Alexa633-LPO (78.7 kDa). After LPO encapsulation, two populations of particles coexist: one with a  $\tau_D$  of 6 ms attributed to LPO-Alexa633-encapsulated vesicles (>85%), and a second with a  $\tau_D$  of 320  $\mu\text{s}$  that corresponds to LPO-Alexa633, which is completely removed by dialysis. On average, a value of  $(8 \pm 5)$  LPO molecules per vesicle was calculated, which represents an encapsulation efficiency of 57% (for an initial concentration of Alexa633-LPO of  $1 \text{ mg mL}^{-1}$ ). The slight decrease in the molecular brightness (from 39 to 34 kHz) has not been included in the estimation of the number of LPO molecules per vesicle.

It is known that LPO interacts with membranes through hydrophobic interactions.<sup>[40,41]</sup> Therefore, to check whether LPO is attached at the vesicles surface we incubated a solution of empty vesicles with Alexa633-LPO (30 nm) and compared it with a solution of Alexa633-LPO-containing vesicles. In the case of empty vesicles, large clusters with diffusion times of up to 30 ms were formed, which revealed that the interaction of Alexa633-LPO with the vesicle surface induces aggregation. Because these aggregates were not detected when Alexa633-LPO was encapsulated inside the vesicles, the enzyme is thus believed to be mainly located inside the polymeric cavity. Presumably, the affinity of LPO to polymer vesicles is responsible for its high encapsulation efficiency, as has already been reported for LPO-containing liposomes.<sup>[42]</sup> Note that the low amount of free enzyme still present after dialysis does not induce clustering. In contrast, SOD was proven to not interact with this type of copolymer and to be located only inside the aqueous cavity of the vesicles.<sup>[23]</sup>

**Coencapsulation of enzymes in nanovesicles:** Because the encapsulation of amphiphilic copolymers during self-assembly is a statistical process, various populations of enzyme-containing vesicles coexist in solution: 1) encapsulated individual enzyme species (either SOD or LPO), 2) coencapsulated enzymes (in various ratios), and 3) empty vesicles (Figure 4C). Testing the efficiency of the system should take these populations into account to avoid a decrease in efficiency resulting from empty vesicles or vesicles containing

individual enzyme species that are not involved in the cascade reaction. The fraction of various populations of vesicles was determined with a combination of FCS and fluorescence cross-correlation spectroscopy, FCCS (Figure 4D). The probability that superoxide radicals escape from the cavity without being detoxified is assumed to be negligible because the disproportionation of superoxide by SOD is one of the fastest observed in biological system.<sup>[35]</sup>

In FCCS, two differently labeled particles provide a positive cross-correlation read-out when bound to each other or located in the same carrier, thus diffusing through the confocal volume in a synchronized way.<sup>[43]</sup> In contrast, the probability of simultaneous movement of freely diffusing fluorophores is so small that it can be neglected. We measured the cross-correlation read-out of the vesicles solution after coencapsulation of Alexa488-SOD and Alexa633-LPO and combined it with FCS data on vesicle populations containing individual enzyme species (Figure 4D). The amplitude of the cross-correlation curve is directly proportional to the number of vesicles containing both enzymes. Under our experimental conditions approximately 10% of the total number of vesicles contained both enzymes and were thus able to participate in the in situ cascade reaction (Supporting Information, Equation (3)). The fraction of 10% of vesicles containing both enzymes is in good agreement with the theoretical fraction of 13%, which represents the total probability of coencapsulation (Supporting Information, Equation (4)). Under the experimental conditions applied, the number of coencapsulated SOD and LPO molecules is relatively small because we intended to minimize interactions and functional changes due to confinement in the nanovesicles. With the selected low concentrations of enzymes (around 8 nm for SOD, and 20 nm for LPO), this cascade enzymatic reaction inside polymeric vesicles allows detection of superoxide radicals with high sensitivity, mimicking natural antioxidant mechanisms. This is very promising as a support to enzyme-based therapeutic applications.

**Activity assay of individual enzyme species in solution and in nanovesicles:** LPO activity (free enzyme and encapsulated within nanovesicles (Supporting Information, Figure S5A and B) was measured by using the formation of highly fluorescent resorufin over time for different amplex red concentrations in the presence of  $\text{H}_2\text{O}_2$ . LPO-containing vesicles without channel proteins inserted in the membrane show no increase in resorufin signal intensity, whereas enzyme-containing vesicles reconstituted with OmpF give a resorufin signal intensity proportional to the initial amplex red concentration. This supports the necessity of channel proteins that allow substrate transport across the polymer wall to maintain the reaction.

Kinetic constants for the enzymatic reaction of LPO ( $K_M$  and  $V_{\text{max}}$ ) were determined using the Lineweaver–Burk equation.<sup>[44]</sup> The slightly lower  $K_M$  value of  $(2.9 \pm 0.1) \mu\text{M}$  compared to free enzyme kinetics  $((9.4 \pm 0.3) \mu\text{M})$  indicates a higher amplex red affinity to LPO in nanovesicles. A higher substrate affinity in encapsulated conditions has been

reported previously.<sup>[6]</sup> This has been explained by the fact that both enzyme and substrate are located at an interface, which provides higher collision frequencies. The maximal reaction rate of the encapsulated enzyme is lower ( $(37.1 \pm 7.1) \mu\text{M s}^{-1}$ ) than in free conditions ( $(132.3 \pm 75.9) \mu\text{M s}^{-1}$ ), but still comparable to the reaction of the free enzyme.

The in situ stability of encapsulated LPO was compared with free LPO over an interval of 60 d (Figure 5A). Between measurements, both free LPO and LPO-containing vesicles were kept in the dark at 4°C. Although the activity decreases significantly down to a maximum of 40% in the case of free enzyme, the enzyme activity inside the nanove-

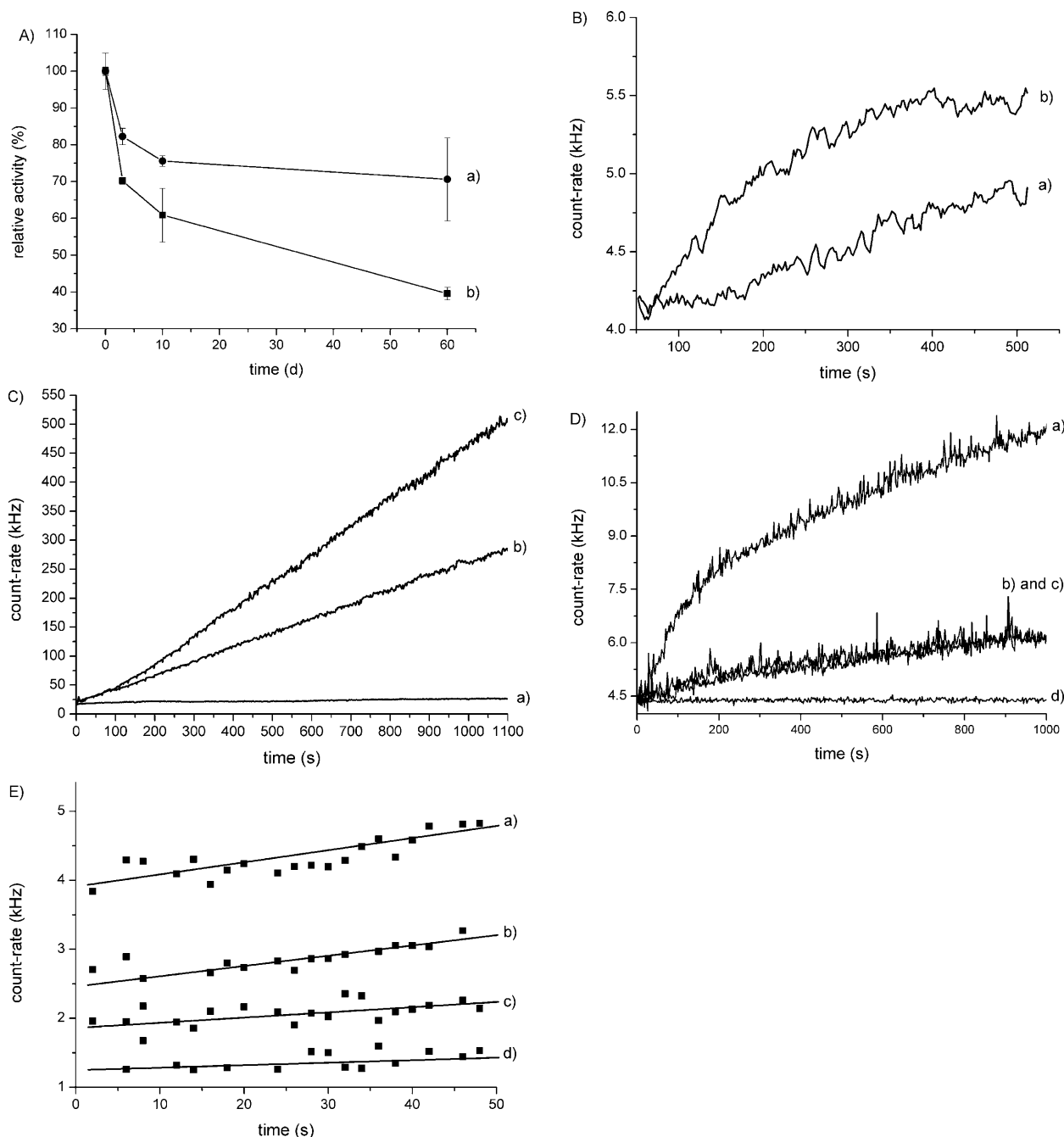


Figure 5. A) LPO activity when encapsulated in polymeric vesicles (a), and in free conditions (b). B) Cascade reaction in free conditions (XA:  $25 \mu\text{M}$ ; XO:  $0.17 \text{ U mL}^{-1}$ ; LPO:  $16 \text{ nM}$ ) in the absence of SOD (a) and in the presence of  $205 \text{ nM}$  SOD (b). Both curves were smoothed by using adjacent-averaging. C) Cascade reaction in free conditions (XA:  $2 \mu\text{M}$ ; XO:  $0.002 \text{ U mL}^{-1}$ ; LPO:  $1 \mu\text{M}$ ) in the absence of SOD (a) and in the presence of  $33 \mu\text{M}$  (b) and  $66 \mu\text{M}$  SOD (c). D) Cascade reaction of SOD-LPO-loaded nanocontainers with OmpF in the polymer membrane (a), SOD-LPO-loaded nanocontainers without OmpF in the polymer membrane (b), LPO-containing vesicles with OmpF in the polymer membrane (c), empty polymer vesicles in the presence of amplex red (d). E) Cascade reaction of SOD-LPO-loaded nanocontainers with OmpF in the polymer membrane and an added amplex red gradient (XA:  $25 \mu\text{M}$ ; XO:  $0.17 \text{ U mL}^{-1}$ ) of  $16.7$  (a),  $8.3$  (b),  $4.16$  (c), and  $1.7 \mu\text{M}$  (d).

sicle is still approximately 70% after 60 d. This represents clear evidence that nanovesicles based on PMOXA-PDMS-PMOXA copolymers provide an advantageous artificial environment for LPO, as already reported for SOD,<sup>[23]</sup> making them suitable for further technological and therapeutic applications.

#### Multienzyme kinetics in a solution that simulates nanovesicle conditions:

It is important to maintain specific enzyme functionality in multienzyme systems to carry out complex reactions as efficiently and as close to nature as possible. Guided by the FCS/FCCS quantitative analysis, we performed activity tests for the SOD–LPO combination in solution by simulating the range of enzyme concentrations expected inside vesicles, and compared them with measurements in the absence of SOD (Figure 5B, curve a). The slope of the curve increases in the presence of SOD (Figure 5B, curve b). Under these conditions, a disproportionation reaction by SOD splits superoxide into hydrogen peroxide that is then consumed by LPO in a further reaction, which allows SOD to work in tandem with LPO. Resorufin formation in the absence of SOD and amplex red autoxidation (Figure 5B, curve a) have been considered as background requiring subtraction at this low enzyme concentration (Figure 5B, curve b). However, these effects are negligible for similar activity tests with high enzyme concentrations (Figure 5C, curve a). Therefore, we compare the kinetics of encapsulated enzymes only to that of free enzymes in a solution that simulates conditions in nanovesicles.

**Multienzyme kinetics in situ inside nanocontainers:** If we consider the case of coencapsulation of SOD and LPO in more detail, we should take into account the requirement that the substrate *S*, specific for the LPO reaction, should be present in proximity to the enzyme to take part in the catalytic reaction for H<sub>2</sub>O<sub>2</sub>. This represents a significant limiting factor because the simultaneous encapsulation of three different molecules increases the statistical complexity of the system and decreases the number of vesicles that contain all components, which introduces difficulties in the detection of the final product of the reaction, resorufin. However, by selecting optimal enzyme concentrations and ratios, when SOD and LPO are coencapsulated in nanovesicles the cascade reaction takes place in situ in the polymer cavity and superoxide anion radicals are successfully reduced to molecular oxygen and water (Figure 5D, curve a). Once formed inside vesicles, the product (resorufin) was detected by fluorescent measurements by using the FCS set-up due to its known high sensitivity and extremely low required concentration in solution; the intensity of the fluorescent signal of resorufin over time was used to calculate enzyme kinetics. Low resorufin formation was exhibited by SOD–LPO-loaded nanovesicles without OmpF (Figure 5D, curve b), attributed to a small amount of non-encapsulated LPO that is capable of oxidizing amplex red in the presence of H<sub>2</sub>O<sub>2</sub> generated by the xanthine/xanthine oxidase system. This is in agreement with the FCS results and indicates that SOD

and LPO are mainly located inside the cavity of the vesicles. A similar effect was seen in the absence of SOD for LPO-containing vesicles reconstituted with OmpF (Figure 5D, curve c). Thus, the side reaction of LPO with the H<sub>2</sub>O<sub>2</sub> generated by the xanthine/xanthine oxidase only represents a background that the high sensitivity resulting from the FCS setup allowed us to detect (Figure 5D, curve c); this differentiates the background from the cascade reaction inside nanovesicles (Figure 5D, curve a). As expected, the copolymer had no effect on amplex red oxidation (Figure 5D, curve d). In SOD–LPO-containing nanovesicles with inserted OmpF (Figure 5D, curve a), a considerable amount of resorufin was formed as compared with vesicles without reconstituted OmpF (Figure 5D, curve b). This clearly indicates that SOD acts in tandem with LPO inside the cavity, in good agreement with the FCCS measurements. Note that statistically, vesicles containing coencapsulated enzymes without OmpF can coexist with those with reconstituted OmpF. However, we calculated that approximately 14 OmpF molecules per vesicles are present in the conditions that we used, which allows us to assume that the amount of vesicles without channel proteins is very low.

Michaelis–Menten kinetics have been already reported to be a suitable model for cascade reactions, such as HRP in the glucose oxidase/horseradish peroxidase tandem.<sup>[45]</sup> It has also been shown that Michaelis–Menten kinetics can be applied at the single-molecule level, even if the signal-to-noise ratio is at the detection limit.<sup>[46]</sup> Therefore, we used a Michaelis–Menten kinetic approach to obtain the kinetic parameters for the cascade reaction under single-molecule conditions in free solution and inside nanovesicles (in bulk: Figure S6, Supporting Information; in nanovesicles: Figure 5E).<sup>[45]</sup> Due to the low enzyme concentrations inside the nanocontainers, which results in a low signal-to-noise ratio, data analysis has been treated thoughtfully, similar to other reported systems of enzymes encapsulated inside vesicles.<sup>[6,8]</sup> In free solution, the Michaelis–Menten constant  $K_M$  was calculated as  $(1.1 \pm 0.1) \mu\text{M}$ , lower than that for nanocontainers  $((7.3 \pm 0.4) \mu\text{M})$ . These values can be rationalized by considering the fact that the population of SOD–LPO-containing nanocontainers is low compared with the other populations of vesicles that contain only one species of enzyme. The latter might induce lower substrate accessibility because H<sub>2</sub>O<sub>2</sub> generated by the SOD-containing vesicles has to be detoxified by the LPO-containing vesicles, which might affect the  $K_M$  value. However, due to the presence of OmpF, the requirement of having an excess of H<sub>2</sub>O<sub>2</sub> at LPO is fulfilled, and in a first approximation it is still possible to model by using Michaelis–Menten kinetics. The values of  $V_{\text{max}}$  ( $V_{\text{max(bulk)}}: 11.1 \mu\text{M s}^{-1}$ ;  $V_{\text{max(nanoprocessor)}}: 0.02 \mu\text{M s}^{-1}$ ) also show the same tendency as presented in LPO single-enzyme kinetics, in which the reaction rate is higher for free-enzyme conditions.

The high stability of polymeric vesicles and their limited miscibility with phospholipids<sup>[47]</sup> allows them to remain structurally intact inside cells over extended periods of time.<sup>[9]</sup> Preliminary results point to both an uptake by cells

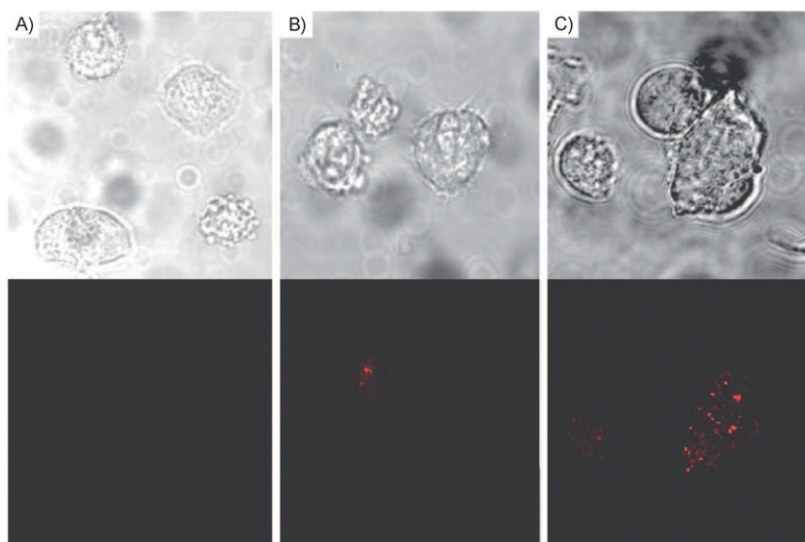


Figure 6. In vitro uptake and activity of SOD–LPO-containing nanocontainers as artificial organelles. A) Transmission and confocal fluorescence image of THP-1 cells preincubated with SOD–LPO-loaded nanocontainers without OmpF, then treated with amplex red and paraquat; B) THP-1 cells preincubated with SOD–LPO-loaded nanocontainers with reconstituted OmpF, then treated with amplex red; C) THP-1 cells preincubated with SOD–LPO-loaded nanocontainers with reconstituted OmpF, then treated with amplex red and paraquat. Confocal fluorescence image of THP-1 cells was corrected with the auto-oxidation background.

of nanocontainers that contain the enzyme combination, as artificial organelles, and to their in vitro functioning by resorufin formation (Figure 6) that is the final step of the sequential SOD–LPO reactions. THP-1 cells incubated with amplex red only exhibit low auto-fluorescence. This was taken to be the background, taken into account, and corrected by using LSM experimental parameters to allow a straightforward detection of resorufin formation that can only be attributed to the presence of nanocontainers that contain the enzyme combination (Supporting Information, Figure S7). THP-1 cells incubated with these artificial organelles show their internalization, and the fluorescence related to resorufin formation reveals that they are active and highly efficient in ROS detection and catalysis inside biological cells (Figure 6B). Incubation of the cells with these artificial organelles and treatment with paraquat, known to produce intracellular superoxide radicals,<sup>[48]</sup> enhanced the intensity of the resorufin fluorescent signal significantly (Figure 6C). THP-1 cells containing enzyme-loaded nanocontainers without OmpF channels did not show any resorufin signal under these conditions because amplex red could not enter the vesicles (Figure 6A).

These results can be explained by the fact that both enzymes are simultaneously located in a polymeric compartment that is made permeable by protein channels, which induces high efficacy into the system. In addition, an excess of superoxide radicals specific to the particular biochemistry of pathological conditions defines the function of these artificial organelles. Thus, they are able to detect ROS and locally degrade them under conditions of oxidative stress.

## Conclusion

We have introduced the concept of enzymatic cascade reactions inside polymeric nanocontainers to combat ROS-induced oxidative stress by simultaneously coencapsulating SOD and LPO, which act in tandem in polymeric vesicles generated by self-assembly of amphiphilic copolymers. Similarly to nature, superoxide anion radicals present in the environment are reduced in situ into molecular oxygen and water via hydrogen peroxide inside the vesicle cavities. In contrast to previous attempts, which involved drastic limitations, such as an uncontrolled release of enzymes, our system allows in situ and instant detection and detoxification of  $O_2^{\cdot-}$  radicals. In addition, activity tests over time have proven

that both enzymes preserve their activity longer than in solution, which makes this system suitable for further technological and therapeutic applications. Given that our superoxide radical processors are fully active even when a small number of enzyme molecules are coencapsulated, and based on a smart fluorescent reply, they are ideal as sensitive biosensors in living cells. To generate homogenous, high-capacity detoxification devices, they were optimized in terms of encapsulation efficiency, concentration, and polydispersity. Despite the many advantages, there is still room and need for further improvements within the concept of artificial organelles production or extension of application to other ROS species. Because this can be achieved by a simple exchange of the enzyme combination, the biosynthetic system is easy to modify for applications in which high adaptability and low costs are important. In addition, further developments will aim at investigating these artificial organelles in various cell lines in detail to specifically address pathological conditions, one of the major objectives in oxidative stress.

## Experimental Section

Experimental details (materials and methods), details of enzyme labeling and purification, channel protein production, preparation and characterization of empty vesicles, individual enzyme-containing vesicles and nanocontainers, light-scattering data, form-factor analysis, TEM micrographs of empty polymer vesicles, an activity assay of LPO in solution, multi-enzyme kinetics in solution, and transmission and confocal fluorescence images of THP-1 cells treated with amplex red and amplex red/paraquat can be found in the Supporting Information.



## Acknowledgements


Financial support was provided by the Swiss National Science Foundation and the National Center of Competence in Nanoscale Science and this is gratefully acknowledged. P. Tanner thanks Jörg Mütze (Technische Universität Dresden) for fruitful discussions covering FCCS. The authors thank Dr. H. Palivan for useful discussions and M. Inglin for reading the manuscript.

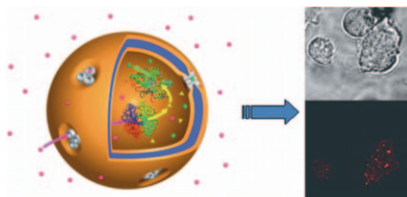
- [1] G. Delaittre, I. C. Reynhout, J. J. L. M. Cornelissen, R. J. M. Nolte, *Chem. Eur. J.* **2009**, *15*, 12600–12603.
- [2] A. Napoli, M. J. Boerakker, N. Tirelli, R. J. M. Nolte, N. A. J. M. Sommerdijk, J. A. Hubbell, *Langmuir* **2004**, *20*, 3487–3491.
- [3] V. Balasubramanian, O. Onaca, R. Enea, D. W. Hughes, C. G. Palivan, *Expert Opin. Drug Delivery* **2010**, *7*, 63–78.
- [4] S. M. Borisov, O. S. Wolfbeis, *Chem. Rev.* **2008**, *108*, 423–461.
- [5] B. V. Rajesh, W. Takashima, K. Kaneto, *React. Funct. Polym.* **2005**, *62*, 51–59.
- [6] Q. Chen, H. Schoenherr, G. J. Vancso, *Small* **2009**, *5*, 1436–1445.
- [7] A. Graff, C. Fraysse-Ailhas, C. G. Palivan, M. Grzelakowski, Th. Friedrich, C. Vebert, G. Gscheidt, W. Meier, *Macromol. Chem. Phys.* **2010**, *211*, 229–238.
- [8] M. Grzelakowski, O. Onaca, P. Rigler, M. Kumar, W. Meier, *Small* **2009**, *5*, 2545–2548.
- [9] N. Ben-Haim, P. Broz, S. Marsch, W. Meier, P. Hunziker, *Nano Lett.* **2008**, *8*, 1368–1373.
- [10] J. R. Henderson, H. Swallow, S. Boulton, P. Manning, C. J. McNeil, M. A. Birch-Machin, *Free Radical Res.* **2009**, *43*, 796–802.
- [11] D. Chen, T. Xi, J. Bai, *Biomed. Mater.* **2007**, *2*, S126–128.
- [12] W. Dröge, *Oxid. Stress Dis. Cancer* **2006**, 885–895.
- [13] A. Lomri, *Future Rheumatol.* **2008**, *3*, 381–392.
- [14] J. E. Slemmer, J. J. Shacka, M. I. Sweeney, J. T. Weber, *Curr. Med. Chem.* **2008**, *15*, 404–414.
- [15] G. Jadot, A. Vaillie, J. Maldonado, P. Vanelle, *Clin. Pharmacokinet.* **1995**, *28*, 17–25.
- [16] R. Igarashi, J. Hoshino, A. Ochiai, Y. Morizawa, Y. Mizushima, *J. Pharmacol. Exp. Ther.* **1994**, *271*, 1672–1677.
- [17] M. M. Gaspar, O. C. Boerman, P. Laverman, M. L. Corvo, G. Storm, M. E. Meirinhos Cruz, *J. Controlled Release* **2007**, *117*, 186–195.
- [18] T. T. Jube, S. Antler, S. Haupt, Y. Barenholz, A. Rubinstein, *Mol. Pharm.* **2005**, *2*, 2–11.
- [19] S. Lee, S. C. Yang, M. J. Heffernan, W. R. Taylor, N. Murthy, *Bioconjugate Chem.* **2007**, *18*, 4–7.
- [20] M. G. P. Saifer, R. Somack, L. D. Williams, *Adv. Exp. Med. Biol.* **1994**, *366*, 377–387.
- [21] Y. Barenholz, *Curr. Opin. Colloid Interface Sci.* **2001**, *6*, 66–77.
- [22] V. R. Muzykantov, *J. Controlled Release* **2001**, *71*, 1–21.
- [23] F. Axthelm, O. Casse, W. H. Koppenol, T. Nauser, W. Meier, C. G. Palivan, *J. Phys. Chem. A* **2008**, *112*, 8211–8217.
- [24] D. E. Discher, A. Eisenberg, *Science* **2002**, *297*, 967–973.
- [25] C. Nardin, S. Thoeni, J. Widmer, M. Winterhalter, W. Meier, *Chem. Commun.* **2000**, 1433–1434.
- [26] D. M. Vriezema, M. Comellas Aragonès, J. A. A. W. Elemans, J. J. L. M. Cornelissen, A. E. Rowan, R. J. M. Nolte, *Chem. Rev.* **2005**, *105*, 1445–1489.
- [27] S. F. M. van Dongen, M. Nallani, J. J. L. M. Cornelissen, R. J. M. Nolte, J. C. M. van Hest, *Chem. Eur. J.* **2009**, *15*, 1107–1114.
- [28] C. H. Coyle, K. N. Kader, *ASAIO J.* **2007**, *53*, 17–22.
- [29] M. Antonietti, S. Foerster, *Adv. Mater.* **2003**, *15*, 1323–1333.
- [30] P. Broz, S. Driamov, J. Ziegler, N. Ben-Haim, S. Marsch, W. Meier, P. Hunziker, *Nano Lett.* **2006**, *6*, 2349–2353.
- [31] M. Kumar, M. Grzelakowski, J. Zilles, M. Clark, W. Meier, *Proc. Natl. Acad. Sci. USA* **2007**, *104*, 1–6.
- [32] O. Onaca, D. W. Hughes, V. Balasubramanian, M. Grzelakowski, W. Meier, C. G. Palivan, *Macromol. Biosci.* **2010**, *10*, 531–538.
- [33] R. Koebnik, K. P. Locher, P. Van Gelder, *Mol. Microbiol.* **2000**, *37*, 239–253.
- [34] C. Nardin, J. Widmer, M. Winterhalter, W. Meier, *Eur. Phys. J. E* **2001**, *4*, 403–410.
- [35] E. Michel, T. Nauser, B. Sutter, P. L. Bounds, W. H. Koppenol, *Arch. Biochem. Biophys.* **2005**, *439*, 234–240.
- [36] K. D. Kussendrager, A. C. M. Van Hooijdonk, *Br. J. Nutr.* **2000**, *84*, 19–25.
- [37] O. Stauch, R. Schubert, G. Savin, W. Burchard, *Biomacromolecules* **2002**, *3*, 565–578.
- [38] M. Eigen, R. Rigler, *Proc. Natl. Acad. Sci. USA* **1994**, *91*, 5740–5747.
- [39] P. Rigler, W. Meier, *J. Am. Chem. Soc.* **2006**, *128*, 367–373.
- [40] T. J. Halthur, T. Arnebrant, L. Macakova, A. Feiler, *Langmuir* **2010**, *26*, 4901–4908.
- [41] I. E. Svendsen, L. Lindh, T. Arnebrant, *Phys. Chem.* **2007**, *221*, 65–73.
- [42] J. P. Colletier, B. Chaize, M. Winterhalter, D. Fournier, *BMC Biotechnol.* **2002**, *2*, 9.
- [43] P. Schwille, F. J. Meyer-Almes, R. Rigler, *Biophys. J.* **1997**, *72*, 1878.
- [44] A. Cornish-Bowden in *Fundamentals of Enzyme Kinetics*, 3rd ed., Portland, London, **2004**, Chapter 5.
- [45] Z. Zhu, C. Momeu, M. Zakhartsev, U. Schwaneberg, *Biosens. Bioelectron.* **2006**, *21*, 2046–2051.
- [46] B. P. English, W. Min, A. M. van Oijen, K. T. Lee, G. Luo, H. Sun, B. J. Cherayil, S. C. Kou, X. S. Xie, *Nat. Chem. Biol.* **2006**, *2*, 87–94.
- [47] K. Kita-Tokarczyk, F. Itel, M. Grzelakowski, S. Egli, P. Rossbach, W. Meier, *Langmuir* **2009**, *25*, 9847–9856.
- [48] A. T. Black, J. P. Gray, M. P. Shakarjian, D. L. Laskin, D. E. Heck, J. D. Laskin, *Toxicol. Appl. Pharmacol.* **2008**, *231*, 384–392.

Received: September 28, 2010  
Revised: December 6, 2010  
Published online: ■■■■, 2011

**Nanocontainers**

P. Tanner, O. Onaca,  
V. Balasubramanian, W. Meier,  
C. G. Palivan\* ..... ■■■■-■■■■

 **Enzymatic Cascade Reactions inside Polymeric Nanocontainers: A Means to Combat Oxidative Stress**



**Keeping it together:** Enzymatic cascade reactions inside polymeric nanocontainers (see scheme) are introduced as a new theranostic concept. Two enzymes that act in tandem in the cavities of polymeric vesicles allow the simultaneous detection and detoxification of  $O_2^{\cdot-}$  radicals and related, harmful  $H_2O_2$ . The system behaves as artificial organelles in THP-1 cells.